Integrated Predictive Power Control and Dynamic Channel Assignment in Mobile Radio Systems

Kambiz Shoarinejad, *Member, IEEE*, Jason L. Speyer, *Fellow, IEEE*, and Gregory J. Pottie, *Senior Member, IEEE*

***Abstract*—It is known that dynamic allocation of channels and power in a frequency/time-division multiple access system can improve performance and achieve higher capacity. Various algorithms have been separately proposed for dynamic channel assignment (DCA) and power control. Moreover, integrated dynamic channel and power allocation (DCPA) algorithms have already been proposed based on simple power control algorithms. In this paper, we propose a DCPA scheme based on a novel predictive power control algorithm. The minimum interference DCA algorithm is employed, while simple Kalman filters are designed to provide the predicted measurements of both the channel gains and the interference levels, which are then used to update the power levels. Local and global stability of the network are analyzed and extensive computer simulations are carried out to show the improvement in performance, under the dynamics of user arrivals and departures and user mobility. It is shown that call droppings and call blockings are decreased while, on average, fewer channel reassignments per call are required.**

***Index Terms*—Cellular land mobile radio, dynamic channel allocation, Kalman filters, power control.**

I. Introduction

With the ever-increasing need for capacity in mobile radio systems, optimal allocation of resources in nonuniform and nonstationary environments has become a great challenge. The fundamental objective is to accommodate as many users as possible, subject to complexity and quality of service (QoS) requirements, on a limited available bandwidth, by controlling undesired interactions among the users. One major interaction is the cochannel interference that every user generates for all other users which are sharing the same channel. Various techniques have been developed to mitigate the effects of cochannel interference. Some of these techniques, such as sectorization and beamforming using smart antenna arrays, try to suppress interference, while others, such as channel assignment techniques, try to avoid strong interferers.

Another well-known technique is to adaptively control the power levels of all the users in the network. The idea is to keep the power level for every user at its minimum required level according to the current channel conditions. This will eliminate unnecessary interference to other users and will also minimize the power consumption for the user. Various power control algorithms have been proposed in the literature [1]–[12].

Our first objective in this paper is to design a distributed predictive power control algorithm. We try to obtain accurate enough models for the slow variations in the channel gains and the interference powers. We then design Kalman filters for every user to obtain the one-step predicted values for both the interference level and the user's channel gain from its intended base station. We try to tune the filters for a typical mobile radio environment and then conjecture and show through simulations that the filters are indeed robust under a broad range of parameters such as user velocities and shadowing correlation distances. The predicted measurements from the Kalman filters are then used in an integrator algorithm to update the power levels.

Another approach to mitigate the cochannel interference effects and increase the capacity is to avoid strong interferers by dynamically assigning the channels to the users. Various centralized and decentralized dynamic channel assignment (DCA) schemes have been proposed in the literature [13]–[16].

It is believed that an aggressive DCA scheme can make a frequency/time-division multiple access (FDMA/TDMA) system an *interference-limited* system, where the number of active users is mostly limited by the interference that the users cause on each other. On the other hand, power control schemes are known to be especially effective for interference-limited systems. This has initiated research on integrated distributed dynamic channel and power allocation (DCPA) schemes [17]–[20]. In [17], a pilot-based minimum interference DCA scheme is integrated with a fast fixed-step power control algorithm, while fast fading and user mobility effects are neglected. In [18], three different types of minimum interference DCA algorithms are integrated with a slow integrator power control algorithm. Pedestrian mobility along with a low power update rate are considered, and it is again assumed that the fast-fading effects are averaged out. In [19], a simulation study has been performed to investigate the joint effects of some simple signal-to-interference-plus-noise ratio (SIR)-based and signal-level-based power control algorithms along with a minimum interference channel reassignment scheme. Fast-fading effects are again neglected, and low power update rates are assumed.

Most DCPA schemes, however, only consider simple power control algorithms. Moreover, except for [18] and [19], other results neglect such effects as dynamics of user arrival or departures, user mobility, and base station handoffs. Our main objective, in this paper, is to investigate the performance of our predictive power control algorithm when it is integrated with a

Manuscript received August 26, 2001; revised February 18, 2002; accepted February 11, 2003. The editor coordinating the review of this paper and approving it for publication is Y.-B. Lin. This work was supported in part by the Air Force Office of Scientific Research under Grant F49620-00-1-0154.

K. Shoarinejad is with Innovics Wireless Inc., Los Angeles, CA 90064 USA (e-mail: kambiz@innovicswireless.com).

J. L. Speyer is with the Mechanical and Aerospace Engineering Department, University of California at Los Angeles, Los Angeles, CA 90095-1597 USA.

G. J. Pottie is with the Electrical Engineering Department, University of California, Los Angeles, CA 90095-1594 USA.

Digital Object Identifier 10.1109/TWC.2003.817418

minimum interference DCA scheme. We set up a system-level simulation platform, similar to the ones presented in [17] and [18], to compare our predictive DCPA scheme with the one that uses a simple integrator power control algorithm with no prediction. Dynamics of user arrivals and departures, user mobility, and base station handoffs are all considered in this study. Slowly varying flat Rayleigh-fading effects are also considered in the simulations.

The organization of the paper is as follows. In Section II, we present the system model and review some of the results in power control and DCA. In Section III, we elaborate on our predictive power control design. We explain how simple Kalman filters may be designed and implemented in order to obtain the predicted measurements of both the channel gains and the interference powers. We also show that the presented predictive power control algorithm satisfies the sufficient conditions for global stability of the network. In Section IV, we describe in detail our simulation models and, in Section V, we discuss the simulation results and compare the performance of our integrated predictive DCPA algorithm with the corresponding algorithm which uses no prediction. We show that, for a range of traffic loads, the number of blocked calls and dropped calls are decreased under our predictive DCPA scheme. Moreover, on average, fewer number of channel reassignments are required for every call, implying a more stable network. We will provide concluding remarks in Section VI.

II. System Model, Dynamic Channel Assignment, and Power Control

We consider a cellular system where the area under coverage is divided into cells, and each cell has its own base station. All users communicate with their assigned base stations through a single hop. This is in contrast to *ad hoc* wireless networks where there is no fixed infrastructure and multihop communication is prevalent.

We focus on an FDMA/TDMA system and only consider the cochannel interference among the users, i.e., no adjacent channel interference is assumed. Specifically, we assume a system-wide synchronization to the slot level so that each user will experience interference only from the users which are sharing exactly the same slot on the same carrier frequency. This assumption implies that large enough guard times per slot are assumed. We do not consider any blind slots in the system, that is, we assume that any slot in a frame can be used as a traffic channel. Blind slots can be avoided either by appropriate structuring of the control channel or by assuming that a call activity detection scheme is employed such that the users can temporarily discontinue their transmission in their active slots. Modifying the frame structure and considering some slots as the blind slots should not have major effects on our performance comparisons.

We focus on the uplink channel, i.e., the channel from mobiles to base stations. Almost all the results and discussions, however, could similarly be stated for the downlink channel. We assume a fixed-power pilot (control) channel on the downlink. As we shall see, this channel facilitates DCA and can be used by the mobiles for initial base station assignments and base station handoffs.

We abstract the system architecture, as far as modulation, coding, etc., are concerned, and consider SIR as the only measure for QoS in the system. This is a common practice, even though bit-error rate or frame-error rate are usually seen as the ultimate performance measures. The reason is that, in general, higher SIR will result in better bit-error-rate performance and considering SIR as the measure for QoS provides us with a more convenient platform for power control design.

The received SIR on an assigned uplink channel for user i can now be written as

$$r_i = \frac{g_{ii}p_i}{\sum_{j=1,j\neq i}^{M} g_{ij}p_j + \eta_i} \tag{1}$$

where p_i is the transmit power for user i, g_{ii} is the channel gain (or attenuation) from user i to its intended base station (in the linear scale), g_{ij} is the channel gain from user j to the intended base station of user i, and η_i is the receiver noise intensity at the intended base station of user i. Also, M is the total number of users sharing the channel. We now review the minimum interference DCA scheme along with the main approaches for power control.

A. DCA

Under a DCA scheme, all base stations have access to all the channels and dynamically assign the channels to the users based on the current traffic conditions. While DCA schemes are clearly more complicated, they usually result in higher capacity.

We adopt a distributed minimum interference DCA scheme [15]. In this scheme, the new users will be assigned to the idle channels with minimum local mean interference, in the order they arrive. It was shown in [26] that when a new user is admitted to a power-controlled network, the optimal power level for the new user can be written as

$$p_n^* = \frac{I_{n0}}{g_{nn}} \frac{\gamma_n}{1 - \frac{\gamma_n}{\gamma_{\max}}} \tag{2}$$

where γ_n is the SIR threshold that the new user wants to achieve, $\gamma_{\max}$ is the maximum achievable SIR for the new user, and I_{n0} is the local mean interference-plus-noise level at the intended base station of the new user before it is admitted to the network. It is now clear that the minimum interference DCA scheme does indeed result in the minimum transmit power for the new user.

Whenever the local mean SIR for a user drops below a given threshold while the user is transmitting at its maximum power level, a channel reassignment attempt is triggered, and, if possible, the user is reassigned to the idle channel, which currently has the minimum local mean interference. Note that this is a distributed scheme, which, in general, is not globally optimal. Remember that any kind of global optimality in the channel assignments can only be achieved through centralized algorithms, which are usually impractical due to the excessive requirements for processing and also communications among the base stations.

Another issue is call management and admission control. As we shall see, a network should be feasible for every user to be able to achieve its desired SIR threshold. If no admission control is employed, a new user could potentially force the network out if its feasibility region and, hence, result in dropping active

calls. Therefore, an admission control mechanism is needed to adjust the tradeoff between blocking new calls and dropping active calls. In [21], an admission algorithm was presented for a power controlled system, where the new users would increase their powers only in small steps. It was shown how this scheme could protect the quality of active links when new users arrive. Channel probing techniques were later proposed in [22]–[24], where a new user would try to estimate the maximum SIR level that it can achieve by disturbing the network as little as possible. The user will then be admitted only if its maximum achievable SIR is above its desired threshold. Also, a channel-partitioning scheme was presented in [25], where a combination of dynamically allocated and fixed assigned channels are incorporated to develop a rapid distributed access algorithm.

We adopt the simpler threshold-based implicit admission control scheme, presented in [18]. In this scheme, a new user with a desired SIR threshold γ_d will be admitted only if there exists an idle channel, on which it can achieve an SIR threshold $\gamma_{\rm new}$, which is higher than γ_d by a given protection margin. The value of the protection margin for new users should be selected based on the tradeoff between blocking new calls and dropping active calls.

Moreover, a channel-reassignment attempt will be triggered for a user if, while transmitting at the maximum power, its local mean SIR drops below a threshold $\gamma_{\rm min}$, which is lower than γ_d by another given margin. This margin is required to avoid excessive number of channel reassignments. The value of this margin should be selected according to the tradeoff between QoS and the average number of channel reassignments per call. Note that for channel reassignment, it is checked whether the user can achieve γ_d on the idle channel which currently has the minimum interference. Since $\gamma_d < \gamma_{\rm new}$, this scheme clearly favors the active users that are being reassigned to the new incoming users. If a channel reassignment fails, the user stays on its old channel and the reassignment attempt is repeated every reassignment period (as long as $r < \gamma_{\rm min}$ and $p = p_{\rm max}$) until the user is either successfully reassigned or dropped from the network. Finally, a user will be dropped from the network if its local mean SIR drops and stays below a threshold $\gamma_{\rm drop}$ $(< \gamma_{\rm min})$ for a given duration.

B. Power Control

While DCA schemes achieve higher levels of capacity by dynamically distributing the traffic across the channels, power control techniques focus on every channel and try to mitigate the cochannel interference by dynamically adjusting the power levels of the cochannel users at their minimum required levels. Therefore, one can reasonably expect that integrating power control with DCA can achieve even higher levels of capacity, even though the capacity gains may not be exactly additive due to some redundancy between the two schemes [18].

A widely studied approach for power control is the *SIR threshold* approach, presented in [4], where the objective is for the SIR of each user in the network to be above a desired threshold, that is

$$r_i = \frac{g_{ii}p_i}{\sum_{j\neq i} g_{ij}p_j + \eta_i} \geq \gamma_i. \tag{3}$$

A necessary and sufficeint condition for the existence of the optimal power levels p_j^* that satisfy the above set of inequalities is called *feasibility*. In other words, a network of users is called feasible if every user can achieve its desired SIR. It was shown in [4] that a network is feasible if and only if $\rho(\Gamma(Z-I)) < 1$, where $Z = [z_{ij}] = [g_{ij}/g_{ii}], \Gamma = \text{diag}(\gamma_1, \ldots, \gamma_M), U = [u_i] = [(\gamma_i\eta_i)/(g_{ii})]$, I is the identity matrix, and ρ denotes the spectral radius of a matrix. Furthermore, under the feasibility condition, the following simple iterative algorithm, which could be implemented in a distributed manner, would converge to the optimal power levels:

$$\begin{aligned} p_i(n) &= \frac{\gamma_i}{g_{ii}}\left(\sum_{j\neq i} g_{ij}p_j(n-1) + \eta_i\right) = \frac{\gamma_i}{g_{ii}}I_i(n) \\ &= p_i(n-1)\frac{\gamma_i}{r_i(n)} \end{aligned} \tag{4}$$

where $I_i(n)$ is the total interference-plus-noise power at the receiver of the intended base station for user i. Therefore, every user only needs a measurement of its own channel gain and its total interference plus noise in order to update its power level. Note that $I_i(n)$ depends on the power levels of the users during the $(n-1)$th power update period. Also, no extra delays are assumed for processing and propagation. Various generalizations of this algorithms have been presented in the literature. A unified framework along with convergence analysis for some of these algorithms were presented in [5].

In most of these algorithms, it is assumed that all the channel gains stay constant for the duration of the convergence of the algorithm. Therefore, it is implicitly assumed that the fading rate of the channel is much slower than the power update rate. In other words, neither the channel-gain variations due to user mobility and fading, nor the measurement errors are taken into account. It was recently shown in [6] that the optimal powers obtained from the SIR balancing approach, under constant gain assumptions, are very close to the optimal powers that minimize the Rayleigh-fading-induced outage probability for every link.

Some researchers have tried to analyze and possibly modify the power control algorithms to take into account the channel-gain variations and the fading-induced measurement errors. In [7], it was shown how the desired SIR for the users may be scaled up to guard against the user mobility effects. In [8], a simulation study was performed to investigate the user mobility effects on slow integrator power control algorithm. In [9], a modification of the distributed SIR balancing algorithm was proposed, which was less sensitive to SIR measurement errors. Also in [10], stochastic measurements were incorporated in the power control algorithm and it was shown that the power levels converge, in the mean square sense, to the optimal power levels. More recently, it was shown in [11] how a simple Kalman filter may be designed to smooth out the interference measurements. Also in [12], it was mentioned how a minimum-variance power control algorithm may be designed when the channel-gain variations are modeled by filtered white noise sequences. Despite all this effort toward analysis and design of power control algorithms in nonstationary environments, most of the results fail to provide a systematic approach.

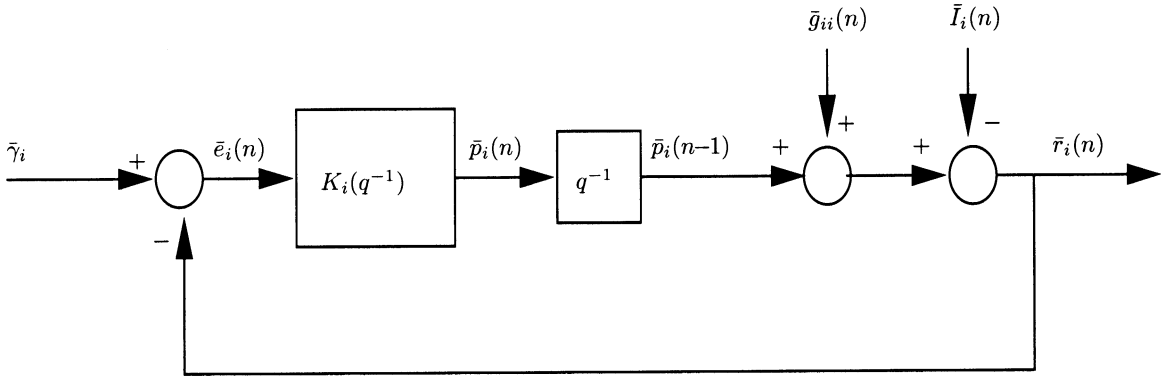

Fig. 1. Local power control loop, associated with a single user.

An alternative approach is to formulate the power control problem as a *decentralized regulator* problem, where the objective is for the SIR of every user to *track* a desired threshold, while the channel gains and the interference levels are changing with time and the SIR measurements can be erroneous. Based on this approach, concepts and design methodologies from control theory have already been used for the analysis of some power control algorithms [27] and design of new algorithms [12], [28].

We first note that, in the logarithmic scale, the distributed iterative algorithm in (4) is a simple unity gain integrator algorithm in a closed-loop. Using a bar on the variables to indicate values in decibels or decibel milliwatts (dBm), we can write

$$\bar{p}_i(n) = \bar{p}_i(n-1) + (\bar{\gamma}_i - \bar{r}_i(n)) := \bar{p}_i(n-1) + \bar{e}_i(n) \tag{5}$$

where $\bar{p}_i(n)$ is the power level in dBm for user i for the duration of the nth power update period and $\bar{r}_i(n)$ is the SIR in decibels for the same user at the beginning of the nth power update period

$$\bar{r}_i(n) = \bar{p}_i(n-1) + \bar{g}_{ii}(n) - \bar{I}_i(n). \tag{6}$$

Moreover, $\bar{I}_i(n)$ is the measured local mean interference-plus-noise power in dBm, available at the beginning of the nth power update period

$$\bar{I}_i(n) = 10\log_{10}\left(\sum_{j\neq i} g_{ij}(n) 10^{\frac{\bar{p}_j(n-1)}{10}} + \eta_i(n)\right). \tag{7}$$

The block diagram for a single loop, associated with a single user, is shown in Fig. 1. The controller transfer function in this case is

$$K_i(q^{-1}) = \frac{\bar{P}_i(q^{-1})}{\bar{E}_i(q^{-1})} = \frac{1}{1-q^{-1}} \tag{8}$$

where q is the shift operator. Therefore, the network can be seen as a set of interconnected local loops. It should be realized that the couplings among the local loops is through the interference function (7), which, in general, is nonlinear. The decentralized regulator formulation of the power control problem can now be presented as the following: *Design a set of local controllers $K_i(q^{-1})$ such that the SIR for every user $\bar{r}_i$ tracks a desired threshold $\bar{\gamma}_i$ with a certain performance while the global network remains stable.*

The local loops in Fig. 1 are quite general and can be modified to accommodate different modeling assumptions. For example, extra delay blocks may be inserted in the feedback path to model processing and propagation delays. Moreover, a saturation block may be inserted in the forward path after the controller to model the maximum and minimum power constraints. Also, we have implicitly assumed a linear time invariant controller by writing $K_i(q^{-1})$. However, in general, the controller itself can be a nonlinear block, as is the case for *fixed-step* power control algorithms. Unfortunately, analysis of stability and convergence of the algorithms, designed via this approach, can be very complicated. Both local and global stability for the network should be analyzed while feasibility of the network and its implications should be addressed.

The global stability of the network implies that all the local loops are stable, but the reverse is not necessarily true. It was shown in [26] that as long as the network stays feasible, i.e., the channel-gain variations do not force the network out of its feasibility region, a sufficient condition for global stability of the network is

$$||G_i(q^{-1})||_{\ell_\infty-\text{induced}} \leq 1 \tag{9}$$

where $G_i(q^{-1})$ is the transfer function from the interference $\bar{I}_i(n)$ to power $\bar{p}_i(n-1)$ and the ℓ_∞-*induced* norm for the single-input–single-output system can be obtained as

$$||G_i(q^{-1})||_{\ell_\infty-\text{induced}} = ||g_i||_1 = \sum_{k=0}^{\infty} |g_i(k)| \tag{10}$$

where g_i denotes the impulse response associated with the transfer function G_i.

Hence, if the local loops are stable, and if the feasibility condition is not violated and (9) is satisfied for all local loops, then the network will be globally stable in the sense that the deviations of the power levels from their corresponding optimal values will always remain bounded. It was also shown in [12] that if the channel gains are constant and the network is feasible (i.e., a fixed optimal power vector $\bar{P}^*$ exists) and if the interference function (7) is linearized around $\bar{P}^*$, then all small deviations of the power levels in the network from their corresponding optimal values will asymptotically converge to zero if

$$||G_i(q^{-1})||_{\ell_2-\text{induced}} = \sup_{\omega} |G_i(e^{j\omega})| \leq 1. \tag{11}$$

The above condition is indeed a sufficient condition for global stability of the linearized network in the ℓ_2-*induced* norm sense, while (9) gives a sufficient condition for global stability in the ℓ_∞-*induced* norm sense without any linearization or any constant gain assumption.

III. Predictive Power Control

Our objective in this section is to show how simple models for the variations in the channel gains and the interference levels may be used in designing simple Kalman filters that provide predicted measurements for both the channel gains and the interference levels while they mitigate the effects of the fast-fading-induced measurement errors.

We are assuming that the received SIR measurement or the power command are sent back to the transmitter. In other words, we are considering *information-feedback* closed-loop power control algorithms. Due to the limitations on the control bandwidth and on the processing time, information-feedback algorithms usually run at slower power update rates. Therefore, similar to DCA algorithms, they operate on the local mean values, which are obtained through some sort of averaging of the measurements over some relatively long periods.

A. Models for Variations in Channel Gains and Interference Levels

The variations in the channel gains can be characterized by the slowly changing shadow-fading and the fast multipath-fading on top of the distance loss. We consider log-normal shadowing whose spatial (or temporal) correlation is represented with a simple first-order Markov model presented in [30].

The channel gain from every user i to its intended base station, in the logarithmic scale, is, therefore, modeled as

$$\bar{g}_{ii}(n) = \bar{g}_{ii}^0 + \delta\bar{g}_{ii}(n) \tag{12}$$

$$\delta\bar{g}_{ii}(n) = a\delta\bar{g}_{ii}(n-1) + w_g(n-1) \tag{13}$$

where $\bar{g}_{ii}^0$ is a constant bias and w_g is a zero mean white Gaussian noise sequence. The constant bias accounts for the antenna gains and the distance loss in the filter. The parameter a is obtained as

$$a = e^{-\frac{vT}{X_s}} \tag{14}$$

where v is the user velocity and T is the update period. Note that vT is the distance that the user moves during one update period. Moreover, X_s is called the shadowing *correlation distance*. It is the distance at which the normalized correlation decreases to e^{-1}. To see this, note that the autocorrelation function for $\delta\bar{g}$ can be obtained as

$$R_{\delta\bar{g}}(m) := E[\delta\bar{g}(m+n)\delta\bar{g}(n)] = \frac{\sigma_{w_g}^2}{1-a^2}a^{|m|} = \sigma_s^2 a^{|m|} \tag{15}$$

where σ_{w_g} denotes the standard deviation of the noise sequence w_g. Note that given the standard deviation for shadowing σ_s and the value for a, the standard deviation for the driving white noise sequence can be obtained.

In order to design distributed algorithms, we need to decouple the local loops in the network. For this purpose, the interference plus noise should be modeled independently for every user. One approach is to treat interference plus noise simply as a bounded disturbance for every user and design the power control algorithm based on the worst case considerations. However, we have decided to model the interference plus noise, similar to the channel gains, by white noise driven first-order Markov variations on top of a constant bias. That is

$$\bar{I}_i(n) = \bar{I}_i^0 + \delta\bar{I}_i(n) \tag{16}$$

$$\delta\bar{I}_i(n) = a\delta\bar{I}_i(n-1) + w_I(n-1) \tag{17}$$

where w_I is a zero-mean white Gaussian noise sequence independent of w_g but with the same variance. While this model may not exactly capture the slow variations in the interference in a power-controlled system, it can still be reasonable when such slow fluctuations in the interference levels are dominated by shadow fading. Note that putting aside the changes in the transmit power levels, due to power control, the fluctuations in the channel gains and interefernce levels basically result from the same physical phenomenon. We, therefore, use this model in a Kalman filter to obtain the one-step predicted measurements of the local mean interference values.

Note that one shall use receiver diversity techniques to combat fast fading since power control algorithms, in general, cannot track very fast channel variations. While we will evaluate the simulated performance of our algorithm with higher power update rates, we have decided to select the power update period such that the fast multipath fluctuations are averaged out while the slower shadowing fluctuations are being tracked. It was shown in [31] that, under the flat Rayleigh-fading assumption, when a first-order lowpass filter, or simply a moving average filter, is used to obtain the local mean values of the measurements, the averaging error in decibels will have a Gaussian distribution, whose mean can be made zero by appropriate choice of the filter dc gain and whose standard deviation depends on the shadow-fading standard deviation σ_s, and the ratio of the shadowing correlation distance to the carrier wavelength X_s/λ, and the normalized measurement time $f_m T$, where $f_m = v/\lambda$ is the maximum Doppler frequency.

It is now clear that the model parameters not only depend on the environment through the values of the shadowing standard deviation and the shadowing correlation distance but also depend on the user velocity. While one can think of implementing individual *adaptive* Kalman filters for each user, where the model parameters are continuously updated based on the available information about the user velocities, we choose to consider a fixed model to design and implement the same filters for all the users in the network. There are two main reasons for this. One is that for a rather broad range of user velocities, the values for a and σ_{w_g}, and as shown in [31], the averaging error variance only slightly change, and we believe that the Kalman filters will be robust to such changes. The other reason is that while some techniques have been already proposed for user velocity estimation in mobile environments (refer to [32] and the references therein), most of them fail to provide accurate estimates in real time.

B. Kalman Filter Design

Using a set of available measurements, corrupted with Gaussian noise, a Kalman filter recursively obtains the minimum mean squared error estimates of a set of variables that are varying according to a given dynamic model. Kalman filters have proved to be strong estimation tools in a very wide range of applications [33]. As examples of applications in communication systems, Kalman filters have been used for channel equalization [34], interference estimation for call admission in CDMA networks [35], and for power control in packet-switched broadband TDMA networks [9].

We propose a predictive power control algorithm, where two Kalman filters are employed to provide the one-step predicted estimates of both the channel gains and the interference levels for every user, which are then used in an integrator algorithm to update the power levels. Using (12) and (13) for the channel gains, we can write

$$\bar{g}_{ii}(n) = a\bar{g}_{ii}(n-1) + (1-a)\bar{g}_{ii}^{0} + w_g(n-1). \tag{18}$$

Similarly, using (16) and (17) for the interference levels, we can write

$$\bar{I}_i(n) = a\bar{I}_i(n-1) + (1-a)\bar{I}_i^{0} + w_I(n-1). \tag{19}$$

The idea is to design two simple Kalman filters that use the erroneous local mean measurements, available to every user, to estimate the constant biases in the models and provide the one-step predicted estimates of the channel gains and the interference levels. As mentioned, the same models are used for all the mobiles in the network. Hence, we eliminate the indexes i and ii for a simpler notation.

It is now appropriate to represent both models in the state-space form. Define $x_{g1}(n) := \bar{g}(n), x_{g2}(n) := \bar{g}^0, x_{I1}(n) := \bar{I}(n)$, and $x_{I2}(n) := \bar{I}^0$. The state-space models for every user can then be obtained as

$$x_g(n) = A_f x_g(n-1) + w_g(n-1) \tag{20}$$
$$y_g(n) = H_f x_g(n) + v_g(n) \tag{21}$$
$$x_I(n) = A_f x_I(n-1) + w_I(n-1) \tag{22}$$
$$y_I(n) = H_f x_I(n) + v_I(n) \tag{23}$$

where

$$x_g := \begin{bmatrix} x_{g1} \\ x_{g2} \end{bmatrix} \quad w_g := \begin{bmatrix} \bar{w}_g \\ w_{g0} \end{bmatrix} \quad w_I := \begin{bmatrix} \bar{w}_I \\ w_{I0} \end{bmatrix} \tag{24}$$

$$A_f := \begin{bmatrix} a & 1-a \\ 0 & 1 \end{bmatrix} \quad H_f := \begin{bmatrix} 1 & 0 \end{bmatrix} \tag{25}$$

where w_{g0} and w_{I0} are two mutually independent *fictitious* zero mean white Gaussian noise sequences, which are also independent from w_g and w_I. They are required to make the filters more robust to the uncertainties in the models. Moreover, v_g and v_I are mutually independent zero mean white Gaussian noise sequences, which are assumed to be independent from all other noise sequences in the model and are used to model the fast-fading-induced averaging errors and other possible uncertainties in the local mean measurements. Remember that all the variables are expressed in a logarithmic scale.

Now, starting from initial estimates $\hat{x}_g(0)^-$ and $\hat{x}_I(0)^-$, the *measurement update* equations for the filters are expressed as

$$\hat{x}_g(n)^+ = \hat{x}_g(n)^- + L_g(n)(y_g(n) - H_f\hat{x}_g(n)^-) \tag{26}$$
$$\hat{x}_I(n)^+ = \hat{x}_I(n)^- + L_I(n)(y_I(n) - H_f\hat{x}_I(n)^-) \tag{27}$$

where $\hat{x}_g(n)^-$ and $\hat{x}_I(n)^-$, respectively, denote the *propagated* (*a priori*) estimates of the channel gain and the interference level at the end of the $(n-1)$th power update period. Hence, at time n (i.e., the beginning of the nth power update period), the current local mean measurements $y_g(n)$ and $y_I(n)$ are incorporated to obtain the *updated* (*a posteriori*) estimates $\hat{x}_g(n)^+$ and $\hat{x}_I(n)^+$. The two-dimensional filter gain vectors L_g and L_I are obtained as

$$L_g(n) = P_g(n)^- H_f^T \left(H_f P_g(n)^- H_f^T + V_g\right)^{-1} \tag{28}$$
$$L_I(n) = P_I(n)^- H_f^T \left(H_f P_I(n)^- H_f^T + V_I\right)^{-1} \tag{29}$$

where V_g and V_I are the measurement noise covariances and $P_g(n)^-$ and $P_I(n)^-$ are the *propagated* estimation error covariance matrices. Note that we only have scalar measurements and no matrix inversion is involved. At time n, the covariance matrices are updated as

$$P_g(n)^+ = P_g(n)^- - L_g(n)H_f P_g(n)^- \tag{30}$$
$$P_I(n)^+ = P_I(n)^- - L_I(n)H_f P_I(n)^-. \tag{31}$$

Now, the one-step predicted estimates for the channel gain and the interference level are obtained by propagating the estimates to the next power update period

$$\hat{x}_g(n+1)^- = A_f\hat{x}_g(n)^+ \tag{32}$$
$$\hat{x}_I(n+1)^- = A_f\hat{x}_I(n)^+ \tag{33}$$

and the covariance matrices are propagated as

$$P_g(n+1)^- = A_f P_g(n)^+ A_f^T + W_g \tag{34}$$
$$P_I(n+1)^- = A_f P_I(n)^+ A_f^T + W_I \tag{35}$$

where W_g and W_I are two-dimensional diagonal covariance matrices for the driving noise sequences in (20) and (22), respectively.

Incorporating the one-step predicted estimates in the integrator algorithm (5), the updated power level for the duration of the nth power update period can be obtained as

$$\bar{p}(n) = \bar{p}(n-1) + (\bar{\gamma} - \hat{\bar{r}}(n+1)^-) \tag{36}$$

where

$$\begin{aligned}\hat{\bar{r}}(n+1)^- &= \bar{p}(n-1) + \hat{x}_{g1}(n+1)^- - \hat{x}_{I1}(n+1)^- \\ &= \bar{p}(n-1) + \hat{\bar{g}}(n+1)^- - \hat{\bar{I}}(n+1)^-.\end{aligned} \tag{37}$$

When a call is assigned (or reassigned) to an idle channel, its Kalman filter estimates are initialized (or reset) as $\hat{x}_{g1}(0)^- = \hat{x}_{g2}(0)^- = \bar{g}(0)$ and $\hat{x}_{I1}(0)^- = \hat{x}_{I2}(0)^- = \bar{I}(0)$, where $\bar{g}(0)$ and $\bar{I}(0)$ are the local mean channel gain and interference values available at the time of channel assignment. Also, the error covariance matrices are initialized as $P_g(0)^- = P_I(0)^- =$

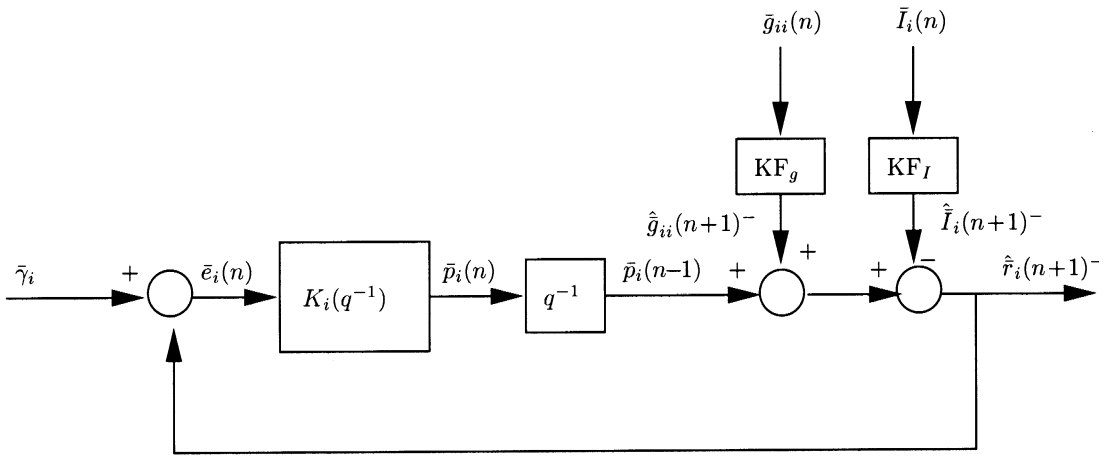

Fig. 2. Local power control loop with Kalman filters.

$\mathrm{diag}(\sigma_s^2, \sigma_s^2)$, where σ_s is the shadow-fading standard deviation (set to 8 dB in our simulations).

We pick the model parameter a according to (14) and by considering the maximum user velocities that we expect in our mobile environment. This makes the filter assume the least correlation among the local mean values in two consecutive power update periods and, therefore, rely more on the measurements. As we shall explain in our simulation details, we assume the power levels to be updated every 100 ms for most of our simulations. Also, we consider the shadowing correlation distance to be about 40 m and the maximum user velocity to be 80 km/h. Using (14), we then pick $a = 0.95$. Using this value for a and $\sigma_s = 8$ dB and (15), we get $\sigma_{w_g}^2 = \sigma_{w_I}^2 = 1.56$. We choose to set $\sigma_{w_g}^2 = \sigma_{w_I}^2 = 2.0$ in the filter, again to deal with uncertainties in the models. The variances for the fictitious driving noise sequences w_{g0} and w_{I0} are also set to 2.0 dB[2]. Also, the standard deviations for the local mean measurement errors are both set to 3.0 dB, i.e., $V_g = V_I = 9.0$.

One should observe that the error covariance matrices and the filter gains are independent of the actual measurements. This can be seen from the filter equations (28)–(35). Therefore, the filter gains L_g and L_I can, in fact, be calculated and saved *a priori*. This can result in a significant reduction in the filter processing time.

Also note that when the filter reaches the steady-state on a specific channel, the steady-state filter gain vectors are equal to

$$L_g = L_I = PH_f^T \left(H_f P H_f^T + V\right)^{-1} \tag{38}$$

where $V_g = V_I = V$ and P is the positive-definite solution to the following *discrete Riccati* equation:

$$P = A_f P A_f^T - A_f P H_f^T (H_f P H^T + V)^{-1} H_f P A_f^T + W \tag{39}$$

where $W_g = W_I = W$. Using our selected values, we get

$$L_g = L_I = L = [0.379\,90 \quad 0.371\,21]^T. \tag{40}$$

C. Global Stability of the Network

When the Kalman filters are employed, the block diagram for a single loop can be depicted as in Fig. 2. We now show that, in the steady-state, the Kalman filters and, therefore, the local loops are stable.[1] Moreover, the sufficient conditions for global stability are satisfied.

Given the filter gains in (40), it is straightforward to obtain the steady-state transfer functions for the Kalman filters

$$\frac{\hat{\bar{g}}(n+1)^-}{\bar{g}(n)} = \frac{\hat{\bar{I}}(n+1)^-}{\bar{I}(n)} = \frac{q(0.379\,47q - 0.360\,91)}{q^2 - 1.570\,53q + 0.589\,09}. \tag{41}$$

The poles of the Kalman filters (i.e., the poles of the above transfer function or equivalently the eigenvalues of $A_f - A_f L H_f$) are located inside the unit circle at

$$s_{f1} = 0.619\,28, \quad s_{f2} = 0.951\,25. \tag{42}$$

It is now clear that all the local loops are stable, i.e., the poles for all the closed-loop transfer functions, associated with a single loop, are inside the unit circle. Processing and propagation delays (i.e., extra delay blocks in the feedback path) could result in instability of the local loops and, therefore, instability of the whole network. However, even though some delay compensation schemes have been proposed in [12], information-feedback power control algorithms, as mentioned before, usually run on lower power update rates, and processing and propagation delays are usually much lower than a power update period.

As we mentioned, stability of the local loops is necessary but not sufficient for global stability of the network. However, the network will indeed be globally stable in the ℓ_∞-*induced* norm sense, if the transfer function from the interference $\bar{I}(n)$ to the power $\bar{p}(n-1)$ satisfies the norm condition (9).

Using (41) and from Fig. 2, it is straightforward to obtain

$$G(q) = \frac{\bar{p}(n-1)}{\bar{I}(n)} = \frac{0.379\,47q - 0.360\,91}{q^2 - 1.570\,53q + 0.589\,09} \tag{43}$$

[1]Under the technical conditions of stabilizability and detectability, the steady-state Kalman filters are always known to be stable [33].

and, hence, we get

$$||G(q)||_{\ell_2-\text{induced}} \simeq ||G(q)||_{\ell_\infty-\text{induced}} = 1.0. \quad (44)$$

Therefore, $G(q)$ satisfies both (9) and (11). From (9), we conclude that, as long as the network is in its feasible region, the deviations of the power levels of all the users in the network from their corresponding optimal values will always remain bounded. Moreover, from (11), we conclude that if the power levels only slightly deviate from their optimal values, while the channel gains remain constant, they will asymptotically converge back to their optimal values. This proves the global stability of the network, on every channel, both in ℓ_∞ sense and in ℓ_2 sense (with a linearized interference function), when the Kalman filters are at their steady-state.

When multiple channels are considered and the power control algorithm is integrated with a DCA scheme, the global stability analysis for the network becomes extremely complicated. Average number of channel reassignments per call can be considered as a measure, which can somehow show the level of stability for the network. We show through computer simulations that the average number of channel reassignments per call will be significantly reduced when the Kalman filters are employed in the power control algorithm.

IV. Simulation Model

While the previous theoretical analysis helps in justifying the use of Kalman filters in power control algorithms to deal better with the variations in the channel gains and the interference levels as well as the errors in the local mean measurements, a simulation study is essential to analyze the overall performance when such a predictive power control algorithm is integrated with a DCA scheme in a relatively realistic mobile environment. We, therefore, set up a system-level simulation environment, similar to the ones presented in [17] and [18], but on a smaller scale, in order to analyze the overall performance of the network, when our predictive power control algorithm is integrated with a distributed minimum interference DCA scheme. User arrivals and departures and user mobility are all considered. In this section, we explain the details of our simulation platform, and in the next section, we analyze the results.

The simulations run on the frame level, and hence, only power and interference levels are simulated, and no modulation and coding are considered in the simulations. While we do not restrict ourselves to any specific standard, we have tried to stay close to the *global system for mobile communications* (GSM) standard.

A 3×3 square grid of cells is assumed. The base stations are located on the cell centers and are separated by 800 m. To avoid edge effects, a ring simulation structure is assumed, i.e., the statistics are only gathered from the central cell. This is somewhat simpler than a toroidal simulation structure and is shown to provide more optimistic but comparable results [36]. The other reason for our results to be somewhat optimistic is that only nine cells are simulated, and therefore, lower interference levels are generated. However, our simulation results clearly serve our purpose of comparing our predictive DCPA scheme with the one that uses no prediction. Omni-directional antennas with two branch selection diversity is assumed for the base stations.

Every channel is characterized by a pair (m, n), where m denotes the carrier frequency, and n is the index for the time slot. We consider two carrier frequencies and eight slots per carrier. As mentioned before, no blind slots are considered. Hence, there are 16 available channels, all of which can potentially be used as traffic channels.

Every frame is 4.0 ms, consisting of eight slots, each with a duration of 0.5 ms. It is assumed that the signal and interference power measurements for every user are available in every frame at the end of the user's corresponding slot. Various events might then happen every multiple number of frames.

The channel gain for every link is normalized with respect to the base station and mobile antenna gains and is characterized by three components: distance loss, slow or shadow fading, and fast fading. The distance loss is assumed to be inversely proportional to d^α, where α is set to 4.0. For shadowing a log-normal pattern is generated *a priori*. Therefore, the shadowing values only depend on the user's location. The resolution of the shadowing grid is set to be equal to the shadowing correlation distance X_s, which is assumed to be 40 m. The shadowing for every user is then obtained by a normalized bilinear interpolation of the four closest points on the shadowing grid. A slowly varying flat Rayleigh fading is also assumed. This implies that no line-of-sight exists and the delay spread is small compared with the symbol duration or the inverse channel bandwidth and, thus, only a single path with a Rayleigh distributed amplitude (and, hence, exponentially distributed power) can be distinguished. In fact, the Rayleigh-fading component is assumed to be constant for the whole duration of a single slot (0.5 ms). Time correlation for Rayleigh fading is often represented using the Jake's model [29], where it is expressed in terms of a zeroth-order Bessel function of the first kind, which results in a nonrational spectrum. We use a first-order approximation by passing a white complex Gaussian noise through a first-order filter and obtaining the squared magnitude of the output Gaussian process. The time constant of the filter, for every user, is obtained by setting its 3-dB cutoff frequency equal to $f_m/4$, where $f_m = v/\lambda$ is the maximum Doppler frequency for the user [13].

New calls are generated based on a Poisson process with a given arrival rate λ_a. Each call is assigned an exponentially distributed holding time with a given average value T_h. The average *Erlang* load per cell is then obtained as $E_c = \lambda_a T_h / N_c$, where $N_c = 9$ is the total number of cells. The Erlang load per cell effectively determines the average number of users that could be active in every cell at any instant of time. We have considered various combinations of values for λ_a and T_h to simulate the network under different traffic load conditions.

The new users are uniformly distributed in the area. The mobility of the user i is modeled with a constant but random speed v_i and the angle θ_i between the velocity vector and the horizontal axis ($-\pi \leq \theta_i < \pi$). The speed for every new user is selected randomly from a triangular distribution in the range 0–80 km/h. This is preferred over a uniform distribution, as it

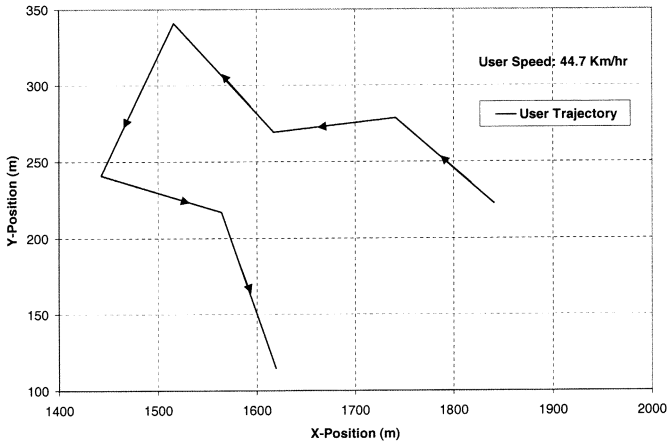

Fig. 3. Sample user motion trajectory.

results in a smaller variance for the velocity distribution among different users. The initial direction θ is uniformly picked. Then, every 10 s, a new direction is selected from a triangular distribution with the old direction as its mean. This is again preferred over a uniform distribution or a two-dimensional random walk, since it makes small angle turns more probable that large ones. The motion trajectory for a sample user is shown in Fig. 3.

The desired SIR threshold for all users in the network is set to $\bar{\gamma}_d = 12$ dB, while the minimum tolerable SIR is considered to be $\bar{\gamma}_{\min} = 10$ dB. Both margins for new user admissions and user droppings are set to 2 dB. Therefore, new users will be admitted only if they can achieve $\bar{\gamma}_{\text{new}} = 14$ dB on the idle channel with the minimum local mean interference. Moreover, a user will be dropped from the network if its SIR drops below $\bar{\gamma}_{\text{drop}} = 8$ dB and stays below for 4.0 consecutive seconds. Note that these margins should have been expressed as percentages of $\bar{\gamma}_d$ and $\bar{\gamma}_{\min}$ for every user, if the users were to have different QoS requirements and, thus, different SIR thresholds.

When a new user arrives into the network, it first starts scanning the downlink control channel from all neighboring base stations and measures all the local mean channel gains. It is assumed that this process take about 0.8 s (200 frames), which is called the initial call setup time. The new user then sends its request for a channel to the base station which has the strongest signal. If this base station does not have any idle channels, the user will try the second best base station. This procedure is called *direct retry* and will be repeated for a given number of base stations (set to three in our simulations) before the user is blocked. When there are idle channels available, the base station checks whether the user can achieve γ_{new} on the idle channel with the minimum local mean interference. If so, the user will be admitted and will be assigned to the idle channel with the minimum interference. Otherwise, the user will be blocked.

We should note that no *macro diversity* is considered, i.e., any user will only communicate with a single base station at any instant of time. Moreover, base station assignment is considered to be separate from power control, i.e., the power levels are obtained assuming that the users are already assigned to their corresponding base stations. Joint base station assignment and power control has already been proposed in the literature [37].

A minimum interference DCA scheme is employed. The local mean channel gain and interference values for possible channel reassignments are obtained by simple averaging of the available measurements over 50 consecutive frames for every user.

Finally, a base station handoff attempt will be triggered if the local mean channel gain from a neighboring base station exceeds the corresponding value from the current base station by a selected handoff margin of 4 dB. If the handoff attempt fails, the user will stay with its current base station. Note that the users are assumed to be continuously monitoring the downlink control channels of all neighboring base stations.

Initially, two power control algorithms are simulated. Specifically, the simple integrator algorithm in (5) and (6) and the predictive algorithm in (36) and (37) are compared. Note that while the propagation simulation models are tailored to individual users, according to their different trajectories and speeds, the same Kalman filter models and parameters are employed for all the users in the network.

After a new user i is admitted, it sets its initial power at

$$p_i(0) = \frac{\gamma_d I_i(0)^-}{g_{ii}(0)^-} \tag{45}$$

where $I_i(0)^-$ and $g_{ii}(0)^-$, respectively, denote the local mean channel gain and the interference-plus-noise level, which are available at the time of user admission. Note that this is somehow an optimistic choice, since a new user sets its initial power as though other users will not increase their transmit powers.

For most of the simulations, the power update rate is assumed to be the same for all users and is set to 100 ms, that is, every user updates its power level every 25 frames. The idea is to have fast multipath fluctuations averaged out while slower variations are being tracked. In all simulations, a maximum transmit power constraint at 30 dBm is imposed on all users in the network, while the receiver noise floor is set to -120 dBm.

It should be mentioned that since the users arrive at arbitrary instants of time according to a Poisson arrival process, the power updates are in fact performed *asynchronously*, even though all the users have the same power update rates. While most results in power control assume synchronous power updates among the users, asynchronous power control algorithms have been addressed in the literature [5]. To have synchronous power updates, one could simply force the users to arrive at instants of time, which are multiples of a common power update period.

V. Performance Analysis

In this section, we present and analyze our simulation results and show how the predictive DCPA scheme can improve the overall performance of the network.

For any given traffic load, we run the simulations multiple times with different random generator seeds and every run continues until enough number of calls are dropped. The statistics are then gathered from the central cell.

Figs. 4 and 5 show the call blocking and the call dropping responses of the network under the two DCPA schemes. It can be seen that at 7.0 Erlang/cell, the predictive DCPA scheme

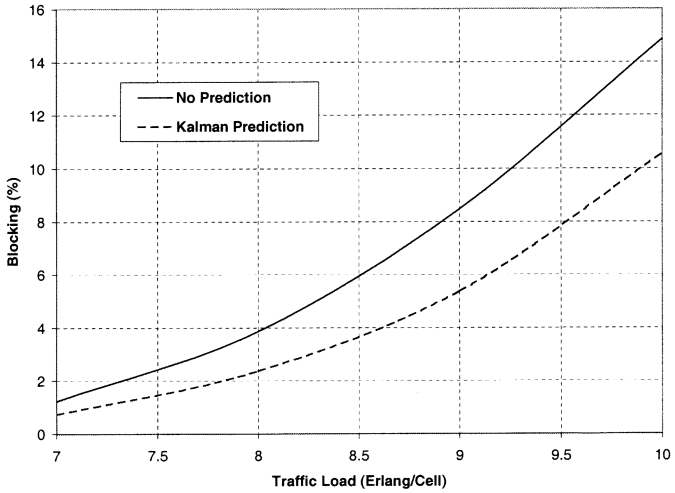

Fig. 4. Call blocking response.

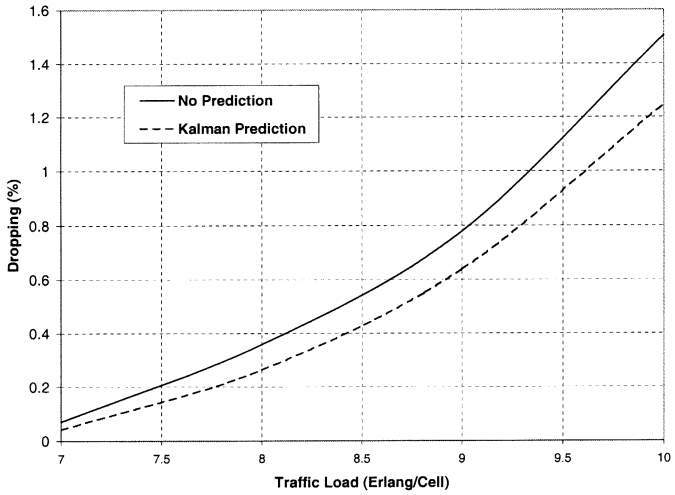

Fig. 5. Call dropping response.

achieves about 0.5% lower blocking rate and about 0.03% lower dropping rate. Moreover, the improvement in performance increases as the traffic load increases. Remember that there is always a tradeoff between blocking new calls and dropping active calls.

Our predictive DCPA scheme also results in better target SIR tracking. We obtain an estimate for the SIR error standard deviation and also estimates for the SIR cumulative distribution functions by looking at the local mean SIR values of all the users in the network at various random instants of time (after enough call attempts have been made and the network has reached some kind of steady state) during every run of the simulation. Fig. 6 shows the standard deviation for the error in the local mean SIR for a range of traffic loads. It can be seen that the predictive scheme decreases the SIR error standard deviation by about 0.3 dB at 7.0 Erlang/cell, while the improvement is about 0.7 dB at 10.0 Erlang/cell. Furthermore, Fig. 7 shows the cumulative distribution for the local mean SIR values in the network under 8.0 and 10.0 Erlang/cell. These figures show how the local mean SIR values for different users are spread around the target SIR value $\gamma_d = 12$ dB. It can be seen that the predictive DCPA scheme results in the local mean SIR values, which are less

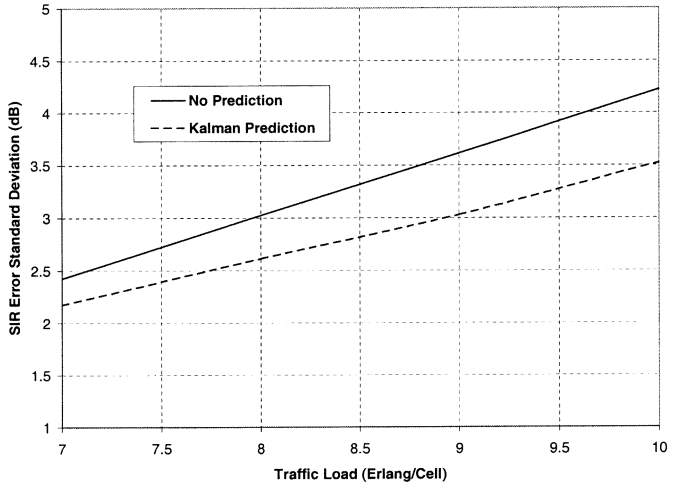

Fig. 6. Standard deviation for the error in the local mean SIR.

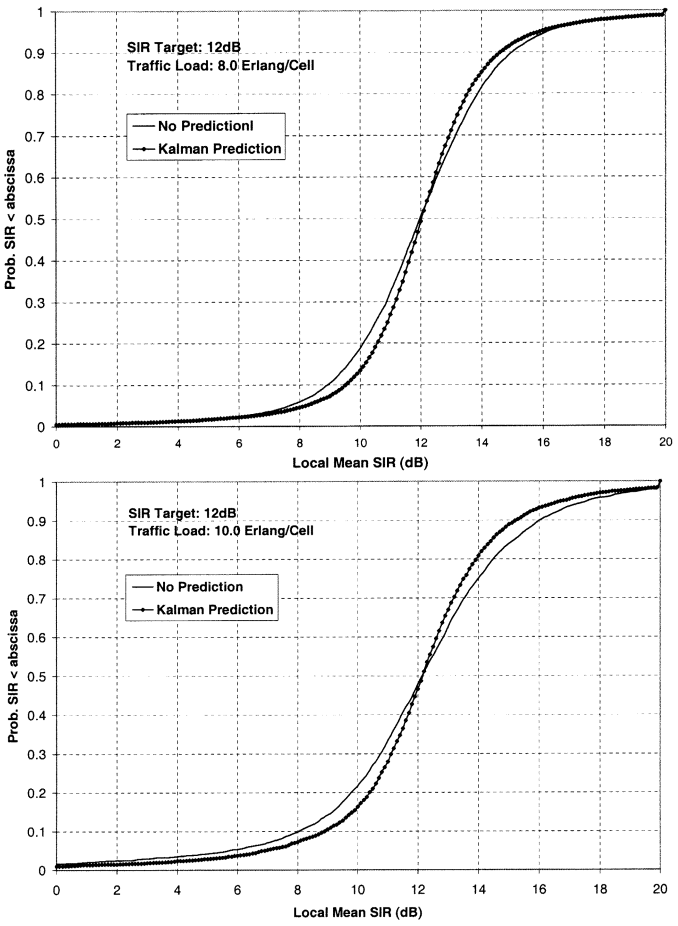

Fig. 7. Cumulative distributions for the local mean SIR.

spread around the target SIR. The improvement is again more noticeable in higher traffic load. In fact, Fig. 8 shows how the local mean SIR cumulative distribution function changes with the traffic load under both schemes.

One measure that shows the level of stability of the network is the average number of channel reassignments per call. Fig. 9 shows this number for a range of traffic loads under both DCPA schemes. As one would expect, fewer channel reassignments

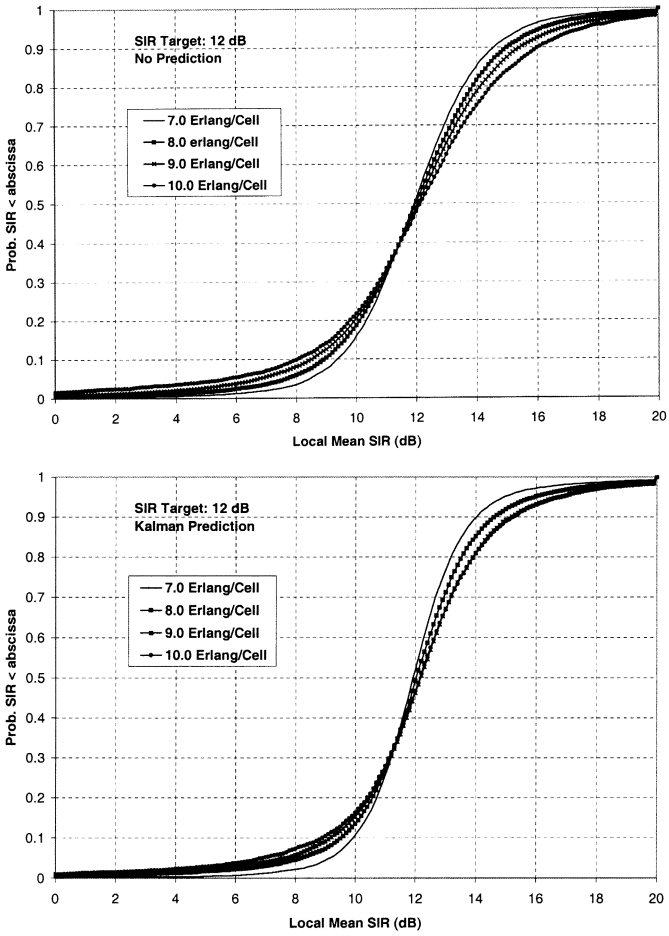

Fig. 8. Traffic load effect on local mean SIR cumulative distribution.

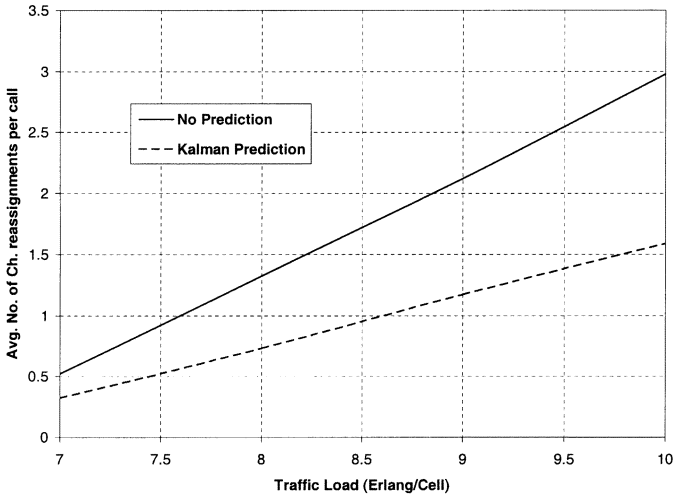

Fig. 9. Average number of channel reassignments per call.

per call are, on average, required in the predictive DCPA scheme. One reason for this is that, as shown before, the predictive scheme does indeed result in better target SIR tracking and smoother local mean SIR behavior.

We also compare the transmit power distribution of the users in the network under the two DCPA schemes. Fig. 10 shows an estimate of the cumulative distribution function for the transmit

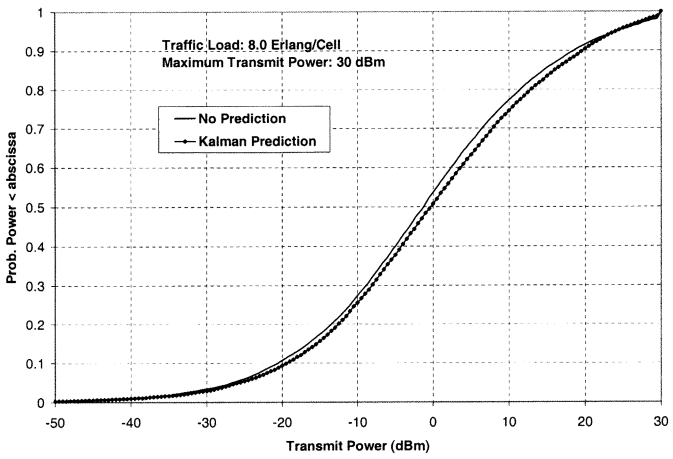

Fig. 10. Transmit power cumulative distribution at 8.0 Erlang/cell.

powers of the users in the network at the load of 8.0 Erlang/cell. It can be seen that the two schemes perform quite similarly, as far as transmit powers are concerned. In fact, both algorithms result in considerable power saving, when compared with a network where all the power levels are fixed at their maximum levels. For example, at a relatively high load of 8.0 Erlang/cell, about 50% of the users under both DCPA schemes are transmitting at 0 dBm or lower power levels. It should, however, be mentioned that our predictive DCPA algorithm seems to result in slightly higher power levels in the network. While one may see this as a small cost for better SIR tracking and better call blocking and dropping responses, it should also be noted that our predictive DCPA scheme does indeed result in higher capacity which in turn implies more active users at any instant in time. This higher traffic explains the higher average transmit power for the users. In fact, Fig. 11 shows how the power cumulative distribution functions might change as the traffic load on the network changes under the two DCPA schemes.

Finally, one might argue that our power update rate is too low for the average speeds considered in our simulations. In order to further evaluate the performance of our predictive algorithm, as compared with standard fast power control schemes, we also simulated the DCPA scheme with standard fixed-step power control algorithm where, depending on the deviation of the received SIR from its target value, the power of each user is incremented or decremented by a fixed 1-dB step every single frame (i.e., once per 4 ms). We then ran the same simulations with our integrated predictive DCPA scheme where the power of each user is updated every fifth frame (i.e., once every 20 ms). Tables I and II show the call dropping and call blocking probabilities for the two scenarios under two sample traffic loads. It can be seen that the results are similar with our predictive algorithm still performing slightly better. Note, however, that while some additional computational cost is associated with our algorithm, the update rate for our algorithm is taken to be five times slower than the standard fixed-step algorithm. We do, however, believe that clarification of the exact tradeoff between the extra computation and the lower update rate would require further analysis using simulations and possibly profiling the code on specific processors.

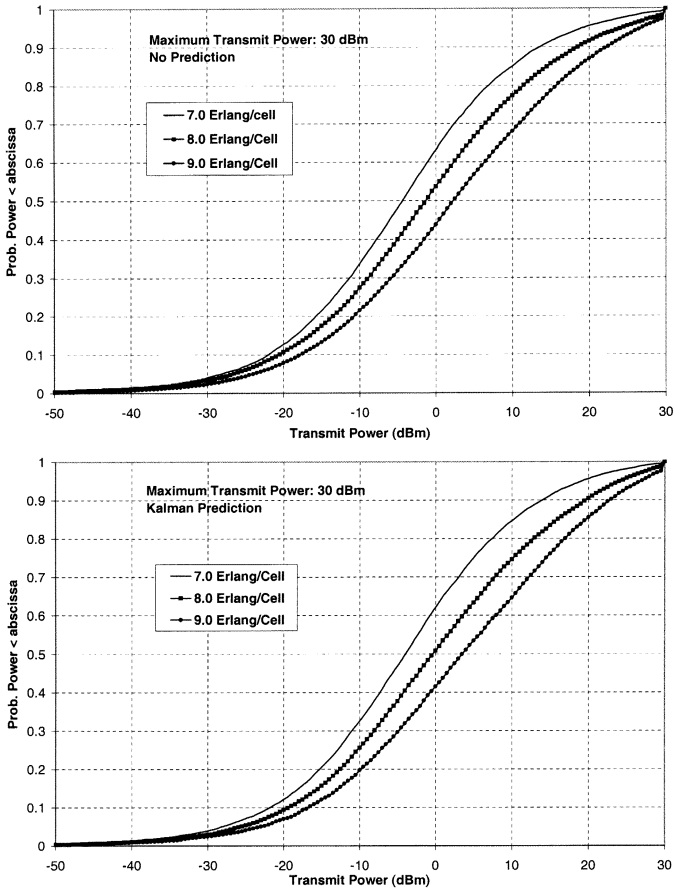

Fig. 11. Traffic load effect on transmit power cumulative distribution.

TABLE I
CALL DROPPING PERCENTAGE

	Fixed-Step DCPA,250 Hz	Predictive DCPA,50 Hz
8.0 Erlang/Cell	0.17%	0.16 %
9.0 Erlang/Cell	0.73 %	0.66 %

TABLE II
CALL BLOCKING PERCENTAGE

	Fixed-Step DCPA,250 Hz	Predictive DCPA,50 Hz
8.0 Erlang/Cell	1.12%	0.86%
9.0 Erlang/Cell	3.27%	3.15%

VI. CONCLUSION

A predictive DCPA scheme has been presented in this paper. Simple Kalman filters were designed to obtain the predicted estimates of the local mean channel gains and the local mean interference-plus-noise levels. These predicted estimates were then incorporated in an integrator algorithm to update the power levels of all the users in the network. It was shown how generic models may be used and filter parameters may be selected to design the same robust filter for all users. Local stability of the network was analyzed. Moreover, it was shown that the sufficient conditions for global stability of the network were satisfied when the Kalman filters were employed in the power control algorithm. The global stability results imply that, as long as the network stays feasible, the deviations of the power levels from their corresponding optimal values will always remain bounded, while the small deviations will always converge back to zero.

This predictive power control algorithm was integrated with a minimum interference DCA scheme in an FDMA/TDMA mobile radio system. A system-level simulation environment was then developed. User arrival and departures and user mobility along with flat Rayleigh-fading effects were all included in the simulations. It was shown that the predictive DCPA scheme results in better call dropping and call blocking responses and also better target SIR tracking performance for the network. Moreover, on average, fewer channel reassignments per call are required under the predictive DCPA scheme. We believe that these improvements are obtained mainly because the predictive algorithm takes into account at least the slow variations of the channel gains. Also, by dealing with uncertainties in the measurements, it effectively mitigates the fading-induced local mean measurement errors. It was also shown that the predictive DCPA scheme results in slightly higher power levels for the users, due to the increased number of simultaneously active users in the network.

As for future research, one may try to design adaptive algorithms where the parameters of the algorithm and even the power update rates are adaptively adjusted for individual users, according to such information as user velocities, etc. Also, the standard integrator algorithm may not be the best power control algorithm. Even though constraints on complexity and computational effort are always present, other simple algorithms may still be designed that could result in better SIR tracking, better allocation of resources, and finally, higher levels of capacity in highly nonuniform and nonstationary environments. Finally, analyzing the behavior of any prediction filter, both in terms of convergence and performance, under bursty interference conditions, can constitute another interesting line of future research.

REFERENCES

[1] J. Zander, "Performance of optimum transmitter power control in cellular radio systems," *IEEE Trans. Veh. Technol.*, vol. 41, pp. 57–62, Feb. 1992.
[2] ——, "Distributed cochannel interference control in cellular radio systems," *IEEE Trans. Veh. Technol.*, vol. 41, pp. 305–311, Aug. 1992.
[3] S. A. Grandhi, R. Vijayan, and D. J. Goodman, "Distributed power control in cellular radio systems," *IEEE Trans. Commun.*, vol. 42, pp. 226–228, Feb./Apr. 1994.
[4] G. J. Foschini and Z. Miljanic, "A simple distributed autonomous power control algorithm and its convergence," *IEEE Trans. Veh. Technol.*, vol. 42, pp. 641–646, Nov. 1993.
[5] R. D. Yates, "A framework for uplink power control in cellular radio systems," *IEEE J. Select. Areas Commun.*, vol. 13, pp. 1341–1347, Sept. 1995.
[6] S. Kandukuri and S. Boyd, "Optimal power control in interference limited fading wireless channels with outage probability specifications," *IEEE J. Select. Areas Commun.*, vol. 1, pp. 46–55, Jan. 2002.
[7] M. Andersin and Z. Rosberg, "Time variant power control in cellular networks," in *Proc. 7th IEEE Int. Symp. Personal, Indoor, Mobile Radio Communications*, vol. 1, Oct. 1996, pp. 193–197.
[8] K. P. Tsoukatos, "Power control in a mobility environment," in *Proc. IEEE Vehicular Technology Conf.*, 1997, pp. 740–744.
[9] Y.-W. Leung, "Power control in cellular networks subject to measurement error," *IEEE Trans. Commun.*, vol. 44, pp. 772–775, July 1996.
[10] S. Ulukus and R. D. Yates, "Stochastic power control for cellular radio systems," *IEEE Trans. Commun.*, vol. 46, pp. 784–798, June 1998.
[11] K. K. Leung, "A Kalman filter method for power control in broadband wireless networks," in *Proc. INFOCOM*, 1999, pp. 948–956.

[12] F. Gunnarsson, "Power control in cellular radio systems: Analysis, design, and estimation," Ph.D. dissertation, Dept. Elect. Eng., Linköping Univ., Linköping, Sweden, 2000.
[13] G. L. Stuber, *Principles of Mobile Communications*. Norwell, MA: Kluwer, 1996.
[14] D. C. Cox and D. O. Reudink, "Dynamic channel assignment in high capacity mobile communication systems," *Bell Syst. Tech. J.*, pp. 1833–1857, Aug. 1971.
[15] D. J. Goodman, S. A. Grandhi, and R. Vijayan, "Distributed dynamic channel assignment schemes," in *Proc. IEEE Vehicular Technology Conf.*, 1993, pp. 532–535.
[16] I. Katzela and M. Naghshineh, "Channel assignment schemes for cellular mobile telecommunication systems: A comprehensive survey," *IEEE Pers. Commun. Mag.*, vol. 3, pp. 10–31, June 1996.
[17] J. C.-I. Chuang and N. R. Sollenberger, "Performance of autonomous dynamic channel assignment and power control for TDMA/FDMA wireless access," *IEEE J. Select. Areas Commun.*, vol. 12, pp. 1314–23, Oct. 1994.
[18] A. Lozano and D. C. Cox, "Integrated dynamic channel assignment and power control in TDMA mobile wireless communication systems," *IEEE J. Select. Areas Commun.*, vol. 17, pp. 2031–2040, Nov. 1999.
[19] R. Verdone and A. Zanella, "On the optimization of fully distributed power control techniques in cellular radio systems," *IEEE Trans. Veh. Technol.*, vol. 49, pp. 1440–1448, July 2000.
[20] G. J. Foschini and Z. Miljanic, "Distributed autonomous wireless channel assignment algorithm with power control," *IEEE Trans. Veh. Technol.*, vol. 44, pp. 420–429, Aug. 1995.
[21] N. D. Bambos, S. C. Chen, and G. J. Pottie, "Radio link admission algorithms for wireless networks with power control and active link quality protection," Elect. Eng. Dept., Univ. California, Los Angeles, CA, Tech. Rep. UCLA-ENG-94-25, 1994.
[22] N. D. Bambos, S. C. Chen, and D. Mitra, "Channel probing for distributed access control in wireless communication networks," in *Proc. GLOBECOM'95*, Singapore, pp. 322–326.
[23] C. C.-Y. Wang, "Power control strategies and variable bit allocation for FH-CDMA wireless systems," Ph.D. dissertation, Elect. Eng. Dept., Univ. California Los Angeles, 1996.
[24] C. J. Hansen, "Probing Techniques for Multiuser Channels with Power Control," Ph.D. dissertation, Elect. Eng. Dept., Univ. California Los Angeles, 1997.
[25] C. J. Hansen and G. J. Pottie, "A distributed access algorithm for cellular radio systems with channel partitioning," *IEEE Trans. Veh. Technol.*, vol. 48, pp. 76–82, Jan. 1999.
[26] K. Shoarinejad, F. Paganini, G. J. Pottie, and J. L. Speyer, "Global stability of feedback power control algorithms for cellular radio networks," in *Proc. 40th IEEE Conf. Decision Control*, vol. 1, 2001, pp. 610–615.
[27] L. Song, N. B. Mandayam, and Z. Gajic, "Analysis of an up/down power control algorithm for the CDMA reverse link under fading," *IEEE J. Select. Areas Commun.*, vol. 19, pp. 277–286, Feb. 2001.
[28] A. El-Osery and C. Abdallah, "Distributed power control in CDMA cellular systems," *IEEE Antennas Propagat. Mag.*, vol. 42, pp. 152–159, Aug. 2000.
[29] W. C. Jakes, *Microwave Mobile Communications*. New York: Wiley, 1974.
[30] M. Gudmundson, "Correlation model for shadow fading in mobile radio systems," *Electron. Lett.*, vol. 27, no. 23, pp. 2145–2146, Nov. 1991.
[31] A. J. Goldsmith, L. J. Greenstein, and G. J. Foschini, "Error statistics of real-time power measurements in cellular channels with multipath and shadowing," *IEEE Trans. Veh. Technol.*, vol. 43, pp. 439–446, Aug. 1994.
[32] R. Narasimhan and D. C. Cox, "Speed estimation in wireless systems using wavelets," *IEEE Trans. Commun.*, vol. 47, pp. 1357–1364, Sept. 1999.
[33] H. W. Sorenson, Ed., *Kalman Filtering: Theory and Application*. Piscataway, NJ: IEEE Press, 1985.
[34] W. Pora, J. A. Chambers, and A. G. Constantinides, "Combination of Kalman filter and constant modulus algorithm with variable step-size for equalization of fast fading channels," *Electron. Lett.*, vol. 34, no. 18, pp. 1718–1719, Sept. 1998.
[35] Z. Dziong, M. Jia, and P. Mermelstein, "Adaptive traffic admission for integrated services in CDMA wireless-access networks," *IEEE J. Select. Areas Commun.*, vol. 14, pp. 1737–1747, Dec. 1996.
[36] W. Ludwin and E. Chlebus, "Performance comparison of simulators for cellular mobile networks," in *Applied Mathematical Modeling*. New York: Elsevier, Aug. 1996, vol. 20, pp. 585–587.
[37] R. D. Yates and H. Ching-Yao, "Integrated power control and base station assignment," *IEEE Trans. Veh. Technol.*, vol. 44, pp. 638–644, Aug. 1995.

Kambiz Shoarinejad (S'96–M'01) received the B.S. and M.S. degrees from the Sharif University of Technology, Tehran, Iran, in 1994 and 1996, respectively, and the Ph.D. degree from the University of California, Los Angeles (UCLA), in 2001, all in electrical engineering.

From 1993 to 1996, he was involved in instrumentation and industrial automation projects with Electric Power Research Center (EPRC) and Atrak Energy Ltd., Tehran. From 1996 to 2001, he was a Teaching and Research Assistant in the Electrical Engineering Department at UCLA where he was involved in research on stochastic decentralized systems with applications in communications and control. During the summer of 1999, he was with Mayflower Communications Corp., Billerica, MA, where he designed and implemented a navigation filter for a differential GPS system. Since March 2001, he has been with Innovics Wireless Inc., Los Angeles, where he is involved in system and algorithm design and embedded firmware development for diversity processing high data rate WCDMA terminals. His general area of interest is in applying stochastic analysis, estimation and filtering, and other system theoretic techniques to applications in communication, control, and navigation systems.

Jason L. Speyer (M'71–SM'82–F'85) received the B.S. degree in aeronautics and astronautics from the Massachusetts Institute of Technology (MIT), Cambridge, in 1960 and the Ph.D. degree in applied mathmatics from Harvard Universtiy, Cambridge, in 1968.

His industrial experience includes research at Boeing, Raytheon, Analytical Mechanics Associates, and the Charles Stark Draper Laboratory. He was the Harry H. Power Professor in Engineering Mechanics at the University of Texas, Austin, and is currently a Professor in the Mechanical and Aerospace Engineering Department, University of California, Los Angeles. He spent a research leave as a Lady Davis Professor at the Technion-Israel Institute of Technology, Haifa, Israel, in 1983 and was the 1990 Jerome C. Hunsaker Visiting Professor of Aeronautics and Astronautics at MIT.

Dr. Speyer has twice been an elected member of the Board of Governors of the IEEE Control Systems Society. He has served as an Associate Editor of the IEEE TRANSACTIONS ON AUTOMATIC CONTROL and as Chairman of the Technical Committee on Aerospace Control. He is a Fellow of the American Institute of Aeronautics and Astronautics.

Gregory J. Pottie (S'85–M'88–SM'01) was born in Wilmington, DE, and raised in Ottawa, ON, Canada. He received the B.Sc. degree in engineering physics from Queen's University, Kingston, ON, in 1984, and the M.Eng. and Ph.D. in electrical engineering from McMaster University, Hamilton, ON, in 1985 and 1988, respectively.

From 1989 to 1991, he worked in the Transmission Research Department of Motorola/Codex, Canton, MA, with projects related to voice band modems and digital subscriber lines. Since 1991, he has been a Faculty Member of the University of California, Los Angeles, Electrical Engineering Department, where he is now Professor and Vice-Chair for Graduate Programs. His research interests include reliable communications, wireless communication systems, and wireless sensor networks. Current projects include design of robust links in mobile networks and investigation of information theoretic issues in sensor networks. He is a cofounder of Sensoria Corporation, Los Angeles, CA.

Dr. Pottie was Secretary to the Board of Governors for the IEEE Information Theory Society from 1997 to 1999. In 1998, he was named the Faculty Researcher of the Year for the UCLA School of Engineering and Applied Science. He is the Deputy Director of the NSF-sponsored Science and Technology Center for Embedded Networked Sensors, and a Member of the Bruin Master's Swim Club (butterfly), and the St. Alban's Choir (2nd bass).